Journal of Power Sources 221 (2013) 128–133

Contents lists available at SciVerse ScienceDirect

Journal of Power Sources

journal homepage: www.elsevier.com/locate/jpowsour

Short communication

Cathodic deposition of $Ni(OH)_2$ and $Co(OH)_2$ for asymmetric supercapacitors: Importance of the electrochemical reversibility of redox couples

Chi-Chang Hu*, Jia-Cing Chen, Kuo-Hsin Chang

Laboratory of Electrochemistry and Advanced Materials, Department of Chemical Engineering, National Tsing Hua University, Hsin-Chu 30013, Taiwan

HIGHLIGHTS

- Reversibility of redox materials determines C_S retention and energy capture efficiency of asymmetric ECs.
- C_S of $Ni(OH)_2$ and $Co(OH)_2$ prepared by cathodic deposition are 2217 and 549 F g^{-1}, respectively.
- $Ni(OH)_2$-graphene is an energy-oriented EC of the asymmetric type.
- $Co(OH)_2$-graphene is a power-oriented EC of the asymmetric type.

ARTICLE INFO

Article history:
Received 20 April 2012
Received in revised form
11 June 2012
Accepted 31 July 2012
Available online 21 August 2012

Keywords:
Cathodic deposition
Nickel hydroxide
Cobalt hydroxide
Supercapacitors
Asymmetric type

ABSTRACT

This work demonstrates the influences of electrochemical reversibility of the pseudocapacitive materials on the performances of an asymmetric supercapacitor consisting of a pseudocapacitive cathode and an anode of the double-layer type. Thanks for the simple, one-step, cathodic deposition of nickel and cobalt hydroxide (denoted as $Ni(OH)_2$ and $Co(OH)_2$, respectively) films from their chloride precursor in aqueous media with the addition of 40 mM NO_3^- as the OH-donating agent. The specific capacitances of $Ni(OH)_2$ and $Co(OH)_2$ films (ca. 0.4 mg cm^{-2}) deposited at 1.0 mA cm^{-2} for 1000 s are equal to 2217 and 549 F g^{-1}, respectively while the electrochemical reversibility of $Co(OH)_2$ is better than that of $Ni(OH)_2$ based on peak potential difference and symmetry of charge/discharge curves. The $Co(OH)_2$-graphene asymmetric supercapacitor shows higher capacitance retention and higher energy efficiency of charge–discharge than the $Ni(OH)_2$-graphene system although the latter system exhibits higher energy and power densities than the former one. The microstructures of as-deposited $Ni(OH)_2$ and $Co(OH)_2$ films have been examined by scanning electron microscopic (SEM), transmission electron microscopic (TEM), and X-ray diffraction (XRD) analyses.

1. Introduction

Electrochemical capacitors (ECs) are widely recognized as an efficient power device complementing primary power sources, such as rechargeable batteries and fuel cells, as well as a buffering/leveling energy storage device of several renewable energy systems, such as wind power and solar cells, because of their high energy efficiency, pulse-/high-power ability, and very long cycle life [1–3]. In fact, ECs become more and more important in the stop-and-go systems which generally require transient but peak-/high-power pulses of charge/discharge for time-dependent usage [4,5] because of their low equivalent series resistance (ESR) for efficiently capturing and storing pulse energy during the braking process [2]. Depending on the power requirement, device size, and energy density, the full charge–discharge time of ECs may range from sub-second (e.g., load-leveling) to hundreds of minutes (e.g., maintenance-free traffic signals) although most commercial available ECs show the ability for full charge in seconds.

According to the charge storage mechanism of devices, ECs have been generally classified into three types: electrical double layer capacitors (EDLCs), redox capacitors (or pseudocapacitors), and asymmetric supercapacitors [1–6]. EDLCs utilize the electrostatic charge separation at the electrolyte–electrode interface to store electric energy which is proportional to the electrolyte-accessible surface area of electrode materials [7]. Redox capacitors consist of electrochemically active materials and employ fast superficial redox reactions [8], which generally show higher energy density in

* Corresponding author. Department of Chemical Engineering, National Tsing Hua University, No. 101, Section 2, Kuang-Fu Road, Hsin-Chu 30013, Taiwan. Tel./fax: +886 3 5736027.
E-mail address: cchu@che.nthu.edu.tw (C.-C. Hu).
URL: http://mx.nthu.edu.tw/%7Ecchu/

0378-7753/$ – see front matter © 2012 Elsevier B.V. All rights reserved.
http://dx.doi.org/10.1016/j.jpowsour.2012.07.111

comparing with EDLCs. However, the energy density of the above symmetric ECs (typically 5–10 Wh kg^{-1} [2]) is much lower than that of rechargeable batteries (e.g., 40 and 160 Wh kg^{-1} for lead-acid and Li-ion batteries, respectively [1,2]). Accordingly, the asymmetrical type consisting of two different electrode materials is designed to overcome the low cell voltage issue of symmetric ECs, especially in the aqueous system, to further promote their energy density [6,9]. Furthermore, ECs of the asymmetric type can be divided into two forms, i.e., the double-layer/redox (e.g., graphene/polyaniline [10]) and redox/redox (e.g., RuO_2/WO_3 [11]) types since the asymmetric design indicates that the electroactive materials in the positive electrode are different from that in the negative one. Unfortunately, significant decrease in the power density and/or cycle-life is commonly found for the asymmetric design [6,9] and how to circumvent a compromise among energy density, power density, and cycle life of asymmetric ECs is a new issue although the energy density of such next-generation ECs is expected to approach that of certain rechargeable batteries.

The above tradeoff in specific power of the asymmetric design is attributable to the fact that the electrochemical reversibility of several electroactive materials proposed for the asymmetric ECs does not meet the basic reversibility requirements for the electrode materials of pseudocapacitors. This issue seems to be apparently circumvented by using the electrode materials with double-layer charge/discharge responses at another electrode because of the excellent reversibility in the double-layer charging/discharging process. However, what will be the outcome of such combination, which needs to be evaluated! Furthermore, the lower electrochemical reversibility of redox materials might significantly increase the ESR of resultant asymmetric ECs, leading to a lower energy-capturing efficiency in storing pulse energy in the stop-and-go systems. Here, we employ $Ni(OH)_2$ and $Co(OH)_2$, two typical positive electrode materials widely investigated for the asymmetric ECs but different in electrochemical reversibility, to emphasize the important influences of intrinsic reversibility of electrochemically active materials on the capacitive performances (e.g., capacitance retention and energy efficiency) of ECs in the asymmetric design. This concept is applicable to all combinations of electrode materials for the asymmetric ECs. Moreover, based on this understanding, the intrinsic characteristics of asymmetric ECs have to be evaluated before recommending their power-/energy-oriented applications (e.g., load-leveling and maintenance-free traffic signals, respectively).

2. Experimental

$Ni(OH)_2$ (or $Co(OH)_2$) was cathodically deposited onto pre-treated graphite substrates from a simple deposition bath containing 40 mM $NaNO_3$ and 20 mM $NiCl_2{\cdot}6H_2O$ (or $CoCl_2{\cdot}6H_2O$) at 70 °C at 1 mA cm^{-2} for 1000 s. Electrochemical deposition of hydroxides was carried out under a three-electrode mode. The pretreatments of the 10 × 10 × 3 mm graphite substrates completely follow our previous procedure [12]. The exposed surface area of every graphite substrate is 10 mm × 10 mm by carefully coating with a thick film of PTFE. After deposition, the PTFE film was removed and the resultant hydroxide/graphite electrodes were rinsed with deionized water for several times and dried in an oven at 85 °C overnight.

Linear sweep voltammograms (LSV), cyclic voltammograms (CV), and chrono-potentiograms (CP) were measured by an electrochemical analyzer (CHI633c, CH Instruments Inc.) in 1 M NaOH (Hanawa EP, Japan). The reference and counter electrodes were Ag/AgCl (Argenthal, 3 M KCl, 0.207 V vs. SHE at 25 °C) and a platinum wire (99.95%, 0.5 mm in diameter and 8 cm in length), respectively. The surface morphologies of hydroxide deposits were examined by a field-emission scanning electron microscope (FE-SEM, Hitachi S4800-type I). X-ray diffraction patterns (not shown here) showed no diffraction peak corresponding to $Co(OH)_2$ and $Ni(OH)_2$, indicating an amorphous structure of both hydroxides, which were obtained from an X-ray powder diffractometer (CuKα, Ultima IV, Rigaku). The nanostructures of hydroxides were examined by a high-resolution transmission electron microscope (HR-TEM, JEM-2010, Joel).

All solutions used in this work were prepared with deionized water produced by a reagent water system (Milli-Q SP, Japan) at 18 MΩ cm. All reagents, not specified, without further purification are Merck, GR. The electrolyte, 1 M NaOH, used for electrochemical characterization was maintained at 25 °C and degassed with purified N_2 for 25 min before measurements. This nitrogen was passed over the solutions during the measurements. The solution temperature was maintained at the specified temperature by a water thermostat (Haake DC3 and K20).

3. Results and discussion

Fig. 1a shows the typical LSV curves measured from 20 mM $CoCl_2{\cdot}6H_2O$ and 20 mM $NiCl_2{\cdot}6H_2O$ with 40 mM $NaNO_3$. The LSV curves measured in both deposition baths are very similar in shape and current density when the potentials are more positive than −0.9 V. This result is reasonably attributed to the fact that

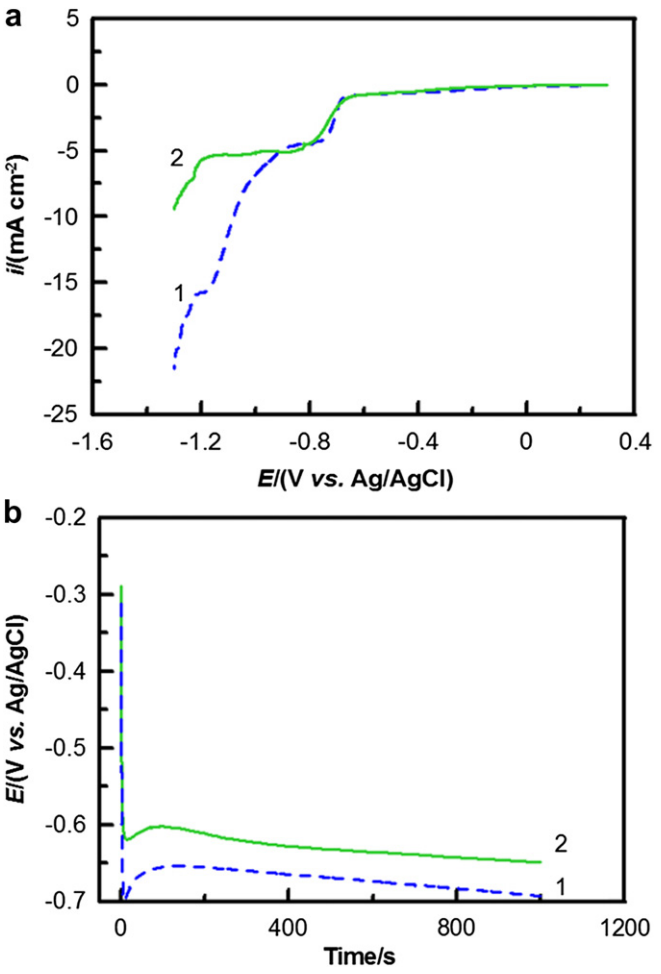

Fig. 1. (a) Linear sweep voltammograms measured at 2 mV s^{-1} and (b) chronopotentiograms obtained at 1 mA cm^{-2} from a solution containing 40 mM $NaNO_3$ and (1) 20 mM $CoCl_2{\cdot}6H_2O$ and (2) 20 mM $NiCl_2{\cdot}6H_2O$ at 70 °C.

reduction of NO_3^- is the main reaction on the first negative sweep for a bare graphite substrate in the above two solutions. Hence, reduction of NO_3^- is not significantly affected by the metallic precursors and significantly occurs at potentials negative to −0.63 V, leading to the deposition of hydroxides. The precipitation of hydroxides at potentials between −0.63 and 0.9 V is believed to result in the different *i*–*E* responses at potentials negative to −0.9 V because different hydroxides and/or oxides might show different catalytic activities for the NO_3^- reduction [13] or hydrogen evolution [14]. Since metallic Ni and Co may be co-deposited with their hydroxides in the very negative potential region (e.g., negative than −0.9 V), the current density for depositing $Co(OH)_2$ and $Ni(OH)_2$ from the above two baths is fixed at 1 mA cm^{-2} to avoid the possible deposition of metallic Ni or Co in the hydroxide films.

Fig. 1b shows the typical chronopotentiograms (CPs) for depositing $Co(OH)_2$ and $Ni(OH)_2$ at 1 mA cm^{-2} from the above two deposition baths. On curve 1, the electrode potentials are sharply moved from the open circuit potential ($E_{OCP} = -0.32$ V) to −0.70 V when the cathodic current is applied; then, the electrode potentials are gradually shifted to a maximum (−0.65 V) with the deposition time reaching 170 s. The first phenomenon is attributable to the double-layer charging effect. The reason responsible for the maximal electrode potential is not clear but is probably due to the natural convection at the electrode–electrolyte interface due to the chemical reaction among Co^{2+} and OH^- as well as the $Co(OH)_2$ precipitation. The electrode potential for depositing $Co(OH)_2$ from this solution slightly varies from ca. −0.65 to −0.69 V in this 1000-s deposition process. On curve 2, the double-layer response is between E_{OCP} and −0.62 V in the deposition solution containing 20 mM $NiCl_2 \cdot 6H_2O$ and 40 mM $NaNO_3$. Comparing with curve 1, the maximal electrode potential is equal to −0.60 V on curve 2 when the deposition time reaches 97 s. A slight decrease from the maximal potential to ca. −0.64 V is found in this 1000-s deposition process. The potential difference for depositing $Co(OH)_2$ and $Ni(OH)_2$ in the 1000-s deposition process is almost constant (0.05 V), suggesting that the electrocatalytic activity of $Ni(OH)_2$ for the NO_3^- reduction is better than that of $Co(OH)_2$.

Fig. 2a and b shows the surface morphologies of $Co(OH)_2$ and $Ni(OH)_2$ deposits, respectively. The surface of $Co(OH)_2$ deposit is rough, which mainly consists of platelets with their diameter in the sub-micrometer range and thickness varying from ca. 50 to 300 nm. Such a microstructure has been observed previously, which was prepared by means of chemical precipitation [15] and electrochemical deposition [16]. This phenomenon is easy to be understood because both chemical precipitation and cathodic deposition involve the combination of Co^{2+} and OH^- to form $Co(OH)_2$ precipitates. In addition, the cathodic deposition of $Co(OH)_2$ and $Ni(OH)_2$ can be simply expressed as follow:

$$M^{2+} + 2OH^- \rightarrow M(OH)_2 \quad (1)$$

where M is indicative of Co and Ni atoms [17]. The morphology of $Ni(OH)_2$ is very rough, which can be considered as a porous network with some large granules (diameter ≈0.6 μm) that can be considered as aggregates of $Ni(OH)_2$ primary particulates. The above observations are further confirmed from the TEM analyses shown in Fig. 2c and d. In fact, the $Co(OH)_2$ platelets can be considered as stacking of several thinner platelets (see Fig. 2c) with their thickness of ca. 15 nm. Moreover, there are several tiny pores randomly distributed on these thin $Co(OH)_2$ platelets, probably due to N_2 bubbling [13]. In Fig. 2d, the size of $Ni(OH)_2$ primary particulates is about 3–5 nm, which may aggregate to large granules or porous network onto the graphite substrate.

Curves 1 and 2 in Fig. 3a show the typical CV curves of $Co(OH)_2$ and $Ni(OH)_2$ deposits measured at 25 mV s^{-1} in 1 M NaOH. On

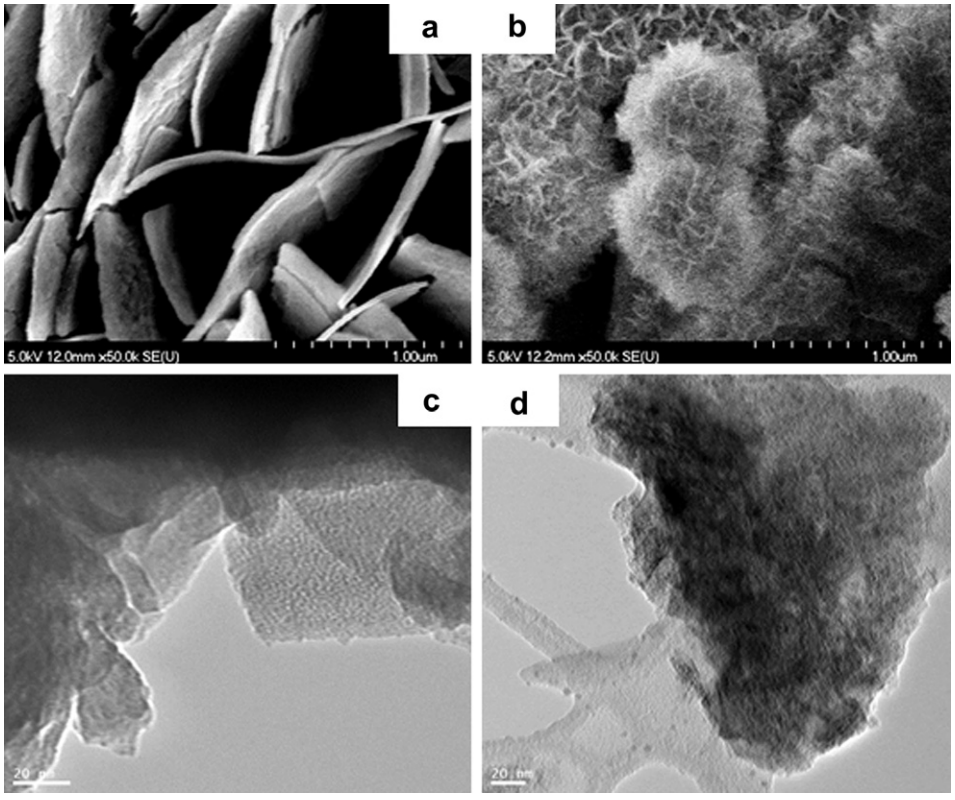

Fig. 2. (a,b) SEM and (c,d) TEM images of (a,c) $Co(OH)_2$ and (b,d) $Ni(OH)_2$ deposits prepared at 1 mA cm^{-2} for 1000 s.

curve 1, a pair of relatively broad, symmetric redox peaks is clearly found. The anodic and cathodic peak potentials are equal to 0.06 and 0.01 V, respectively. The small peak potential difference, ca. 50 mV, indicates a fairly high reversibility of the superficial redox couples (i.e., Co(IV)/Co(III) and Co(III)/Co(II)) in the strong alkaline medium [18]. Moreover, at potentials positive than 0.2 V, a plateau with a potential window of ca. 300 mV on both positive and negative sweeps is clearly found prior to the oxygen evolution reaction. This electrochemical property of $Co(OH)_2$ can be employed as a buffer avoiding gas evolution under a small overcharge situation. On curve 2, a pair of redox peaks corresponding to $NiO_2/Ni(OOH)/Ni(OH)_2$ [19] is clearly found. The peak current densities and voltammetric charges of both peaks on curve 2 are much higher than that on curve 1, revealing a higher charge storage capacity. However, the peak potential difference, ca. 125 mV, is much larger than that on curve 1, indicating a relatively worse reversibility. In fact, this CV curve shows the typical electrochemical behavior of battery-like materials for the positive electrode [1,12], i.e., charging in the higher potential region but discharging in a lower potential region, revealing worse redox reversibility. Since the specific capacitance of $Co(OH)_2$ and $Ni(OH)_2$ is equal to 549 and 2217 F g^{-1}, respectively, more oxy-hydroxyl Ni species can be utilized in the charge storage process in comparison with $Co(OH)_2$. This phenomenon is attributable to that only superficial Co species can be utilized in the charge storage reaction [18,19] while the battery-like materials generally involve the bulk active materials in the charge storage process [1]. On the other hand, specific capacitance of 549 F g^{-1} is fairly high for $Co(OH)_2$, presumably due to the presence of several tiny pores in the thin $Co(OH)_2$ platelets (see Fig. 2c), favorable to the utilization of active oxy-hydroxyl cobalt species. The ultrahigh specific capacitance (2217 F g^{-1}) of $Ni(OH)_2$, a battery-like material, under a low-rate test is not surprising and will approach the theoretical specific capacitance (based on equation (2)) since its discharge potential window is very narrow:

$$C_{th} = \frac{nF}{\Delta V} \quad (2)$$

where C_{th} (>3000 F g^{-1}), n (between 1 and 2), F, and ΔV (=0.5 V) are indicative of the theoretical specific capacitance, electron transfer number of redox couples, Faradaic constant, and potential window of charge–discharge, respectively. The electron transfer number is not integer because of the non-stoichiometric nature of Ni and Co oxy-hydroxyl species [20–23].

Curves 1 and 2 in Fig. 3b shows the capacitance retention against the scan rate of CV for $Co(OH)_2$ and $Ni(OH)_2$ deposits, respectively. Clearly, the specific capacitance of both deposits decreases with increasing the scan rate of CV. This phenomenon is commonly found for pseudocapacitive materials, even $RuO_2 \cdot xH_2O$ [24] (the widely recognized ideal pseudocapacitive material), because the thickness of active materials involving in the redox reactions decreases at a higher scan rate of CV due to a shorter time for ion diffusion. On the other hand, the loss of the specific capacitance for $Co(OH)_2$ is about 46%, which is much smaller than that for $Ni(OH)_2$ (ca. 93%), when the scan rate is increased from 5 to 500 mV s^{-1}. Moreover, the specific capacitance of $Co(OH)_2$ becomes higher than that of $Ni(OH)_2$ when the CV scan rate is higher than 200 mV s^{-1}. The above difference in capacitance retention between $Co(OH)_2$ and $Ni(OH)_2$ reflects the importance of the electrochemical reversibility of superficial redox couples.

Curves 1 and 2 in Fig. 3c show the typical CP curves of $Co(OH)_2$ and $Ni(OH)_2$ at 2 A g^{-1}. From curve 1, the CP curves of $Co(OH)_2$ are highly symmetric, revealing the typical pseudocapacitor behavior with highly electrochemical reversibility. Accordingly, the power ability of $Co(OH)_2$ should be very high and applicable to the power-oriented supercapacitors. For $Ni(OH)_2$, on the other hand, there is a charge plateau and a discharge plateau at ca. 0.35 and 0.27 V, respectively. In both plateau regions, the specific capacitance of $Ni(OH)_2$ is even larger than 10,000 F g^{-1} (e.g., ca. 10,050 F g^{-1} from 0.24 to 0.28 V on the discharge curve). Therefore, $Ni(OH)_2$ (and other battery electrode materials) seems to be the best choice for the electrode materials of supercapacitors because of their extremely high specific capacitance. However, this idea is incorrect! In fact, the extremely ultrahigh specific capacitance of $Ni(OH)_2$ is not surprising because $Ni(OH)_2$ is a typical battery electrode material which commonly shows such results. In developing a battery electrode material, the specific charge capacity (not specific capacitance) in mAh g^{-1}, plateau potentials of charge/

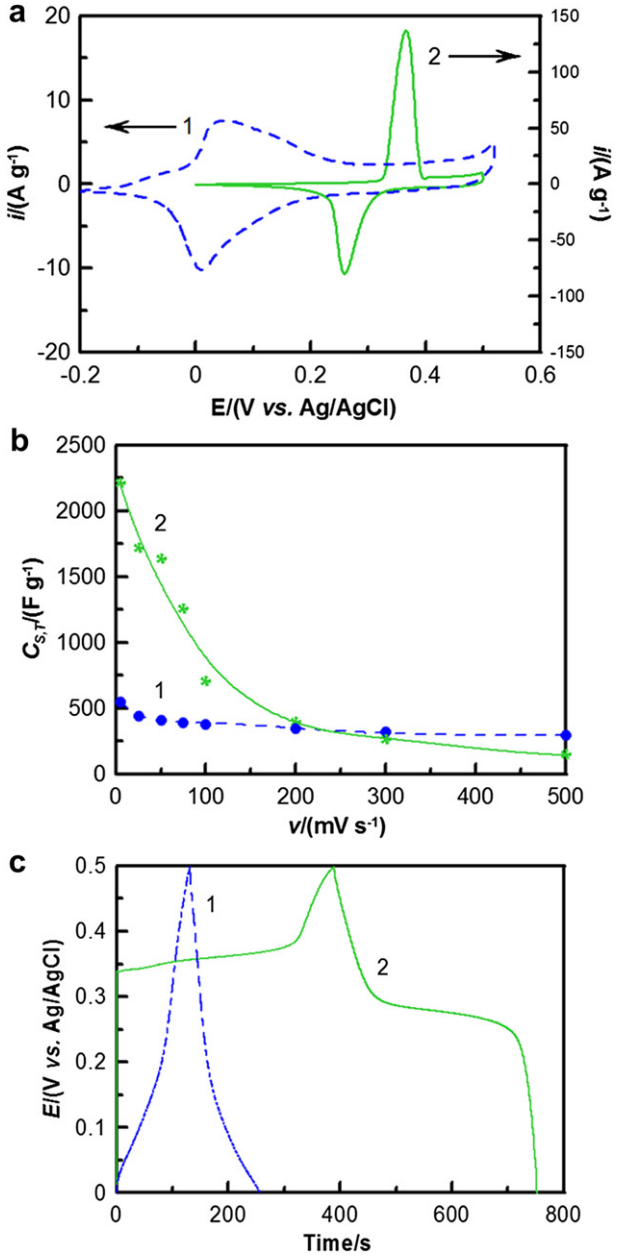

Fig. 3. (a) CV curves measured at 5 mV s^{-1}; (b) capacitance retention against the scan rate of CV, and (c) CP curves measured at 2 A g^{-1} in 1 M NaOH for (1) $Co(OH)_2$ and (2) $Ni(OH)_2$ deposits prepared at 1 mA cm^{-2} for 1000 s.

discharge, and energy density are the main concerns. Based on the potential window of CP curves in Fig. 3c, the electric energy charged into $Ni(OH)_2$ is equal to the area under the charging curve (ca. 80 Wh kg^{-1}) meanwhile the energy delivery from the same electrode is only 57 Wh kg^{-1}. Such significant energy loss not only reduces the capacitive performances but also generates huge heat during charge and discharge processes. The heating effect will render very rapid degradation of electrode materials because the heat capacity of electrolytes in the very limited volume of a cell is low. Therefore, the electrochemical reversibility of superficial redox couples on pseudocapacitive materials has to be carefully considered.

In order to demonstrate the influences of the electrochemical reversibility of the superficial redox couples for pseudocapacitive materials on the performances of ECs in the asymmetric design, the charge–discharge curves of asymmetric ECs with a negative electrode of graphene and a positive electrode of $Co(OH)_2$ and $Ni(OH)_2$ (denoted as cells C and N, respectively) are systematically compared. Typical charge–discharge curves (the 3rd cycle) of cells C and N from 0 to 1.6 V at 4 A g^{-1} are respectively shown as curves 1 and 2 in Fig. 4a. On curve 1, the cell voltage is sharply increased from 0 to ca. 0.3 V when the charging current is applied, attributable to the open-circuit potential difference between graphene and $Co(OH)_2$ and the extremely low background current of $Co(OH)_2$ prior to the redox peaks. Then, the cell voltage is gradually increased with the passed charge, and a quasi-linear voltage–time (V–t) response is visible between 0.3 and 1.55 V, which is the typical capacitor behavior. The relatively asymmetric responses on the charge and discharge at potentials positive than 1.55 V, indicating an irreversible reaction occurs in this cell voltage range, attributable to (minor) gas evolution reactions under a slight overcharging situation. Since the discharge curve is generally symmetric to its charge counterpart and most charges storing in this device can be effectively delivered, the energy and current efficiencies of this device are high (ca. 87 and 90%, respectively). On curve 2, two quasi-linear V–t responses in the potential region of investigation on the discharge curve although the working cell voltage of cell N (between 0.45 and 1.6 V) is somewhat higher than that of cell C. However, the charge curve is not symmetric to its corresponding discharge counterpart for cell N meanwhile the $Ni(OH)_2$-graphene system is charged in a higher cell-voltage region (from 0.59 to 1.6 V) but is discharged in a relatively lower cell-voltage region (from 1.6 to 0.45 V). As a result, both energy and current efficiencies of cell N (73 and 84%, respectively) are lower than that of cell C, demonstrating the significant influences of the redox reversibility of pseudocapacitive materials in such an asymmetric design. In Fig. 4b, the energy efficiencies of cells C and N are monotonously increased with the discharge current density. This phenomenon is due to a higher contribution of an irreversible reaction (after the redox peaks) in the high positive potential region when the charge current density is lower. On the other hand, the energy efficiency of cell C at any specified current density is higher than that of cell N meanwhile the energy efficiencies of cell C at all charge/discharge current densities is above/equal to 80%. From the above results and discussion, the electrochemical reversibility of pseudocapacitive materials in asymmetric ECs of the redox/double-layer type is the key factor determining their energy capture efficiency.

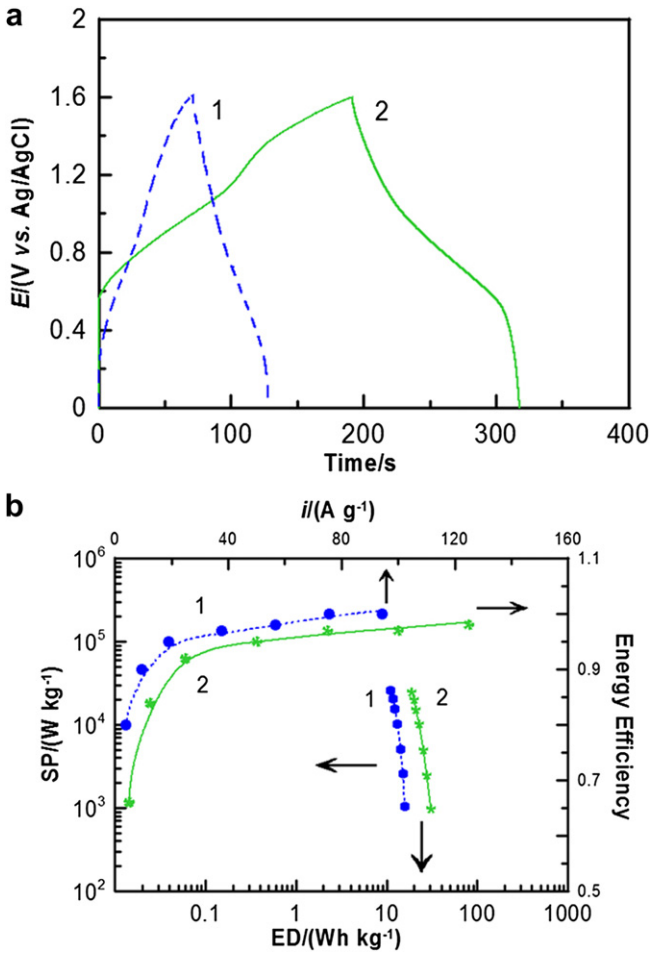

Fig. 4. (a) Charge–discharge curves measured at 4 A g^{-1} in 1 M NaOH and (b) energy efficiency against charge–discharge current density as well as the Ragone plot of (1) $Co(OH)_2$-GS and (2) $Ni(OH)_2$-GS asymmetric supercapacitors.

The Ragone plots of cells C and N obtained from the discharge curves also provide important information. At all discharge current densities, the specific energy of cell C is always lower than that of cell N. This phenomenon is attributed to the higher working cell voltage and higher specific capacitance of $Ni(OH)_2$ in comparison with $Co(OH)_2$. The specific energy of cell N even reaches ca. 30 Wh kg^{-1} under a relatively low power operation (e.g., <1 kW kg^{-1}). Accordingly, cell N is proposed to be an energy-oriented EC of the asymmetric type. Note that when the specific power of discharge is set at 10 kW kg^{-1}, the heat generated by the energy loss of cell N is about 6 Wh kg^{-1}, which is much larger than that of cell C (1.7 Wh kg^{-1}). Accordingly, the joule heating in cell N at a discharge rate of 10 kW kg^{-1} (or higher discharge rates), will sharply increase the cell temperature to an unacceptable level, especially under the repeated operation. Therefore, cell C is proposed to be a power-oriented EC of the asymmetric type although the energy density of cell C is still lower than that of cell N.

4. Conclusions

The electrochemical reversibility of the pseudocapacitive electrode materials is concluded to be the key factor determining the capacitance retention and energy capture efficiency of an asymmetric supercapacitor in the redox/double-layer type, demonstrated by the $Co(OH)_2$-graphene and $Ni(OH)_2$-graphene asymmetric ECs. From the results of capacitance retention, symmetry of charge–discharge curves, and energy efficiency, the $Ni(OH)_2$-graphene and $Co(OH)_2$-graphene systems have been assigned to be the energy- and power-oriented ECs of the asymmetric type. Nanostructured $Ni(OH)_2$ and $Co(OH)_2$, confirmed by the SEM and TEM analyses, with specific capacitance equal to 2217 and 549 F g^{-1}, respectively, have been successfully prepared by

a simple, one-step, cathodic deposition method from an aqueous solution containing their chloride precursor and 40 mM NO_3^- (the OH-donating agent).

Acknowledgments

The financial support of this work, by the Delta-NTHU collaboration program, the National Science Council of Taiwan under NSC100-2628-E-007-028-MY2 and the boost program from Low Carbon Energy Research Center of National Tsing Hua University, is gratefully acknowledged.

References

[1] B.E. Conway, Electrochemical Supercapacitors, Kluwer-Plenum Pub. Co., New York, 1999.
[2] J.R. Miller, A.F. Burke, The Electrochemical Society Interface, Spring, 2008, p. 53.
[3] R. Koetz, M. Carlen, Electrochim. Acta 45 (2000) 2483.
[4] M. Winter, R.J. Brodd, Chem. Rev. 104 (2004) 4245.
[5] S. Nomoto, H. Nakata, K. Yoshioka, A. Yoshida, H. Yoneda, J. Power Sources 97–98 (2001) 807.
[6] J.H. Chae, K.C. Ng, G.Z. Chen, Proc. Inst. Mech. Eng. Part. A-J. Power Energy 224 (A4) (2010) 479.
[7] C.C. Wang, C.C. Hu, Carbon 43 (2005) 1926.
[8] C.C. Hu, C.Y. Hung, K.H. Chang, Y.L. Yang, J. Power Sources 196 (2011) 847.
[9] J.W. Long, D. Belanger, T. Brousse, W. Sugimoto, M.B. Sassin, O. Crosnier, MRS Bull. 36 (2011) 513.
[10] P.J. Hung, K.H. Chang, Y.F. Lee, C.C. Hu, K.M. Lin, Electrochim. Acta 55 (2010) 6015.
[11] K.H. Chang, C.C. Hu, C.M. Huang, Y.L. Liu, C.I. Chang, J. Power Sources 196 (2011) 2387.
[12] C.C. Hu, C.Y. Cheng, J. Power Sources 111 (2002) 137.
[13] C.C. Huang, H.C. Hsu, C.C. Hu, K.H. Chang, Y.F. Lee, Electrochim. Acta 55 (2010) 7028.
[14] T.C. Wen, C.C. Hu, J. Electrochem. Soc. 139 (1992) 2158.
[15] E. Hosono, S. Fujihara, I. Honma, M. Ichihara, H. Zhou, J. Power Sources 158 (2006) 779.
[16] W.J. Zhou, J. Zhang, T. Xue, D.D. Zhao, H.L. Li, J. Mater. Chem. 18 (2008) 905.
[17] Y. Sasaki, T. Yamashita, Thin Solid Films 334 (1998) 117.
[18] C.C. Hu, T.Y. Hsu, Electrochim. Acta 53 (2008) 2386.
[19] C. Lin, J.A. Ritter, B.N. Popov, J. Electrochem. Soc. 145 (1998) 4097.
[20] H. Bode, K. Dehmelt, J. Witte, Electrochim. Acta 11 (1966) 1079.
[21] B.C. Cornilsen, X. Shan, P.L. Loyselle, J. Power Sources 29 (1990) 453.
[22] T.C. Wen, C.C. Hu, Y.J. Li, J. Electrochem. Soc. 140 (1993) 2554.
[23] C.C. Hu, K.H. Chang, T.Y. Hsu, J. Electrochem. Soc. 155 (2008) F196.
[24] C.C. Hu, K.H. Chang, M.C. Lin, Y.T. Wu, Nano Lett. 6 (2006) 2690.